Egyptian Geophysical Society
EGS Journal, Vol. 20, No. 1, 37-49 (2022)

TIME DOMAIN ELECTROMAGNETIC AND GEOELECTRICAL MODELING FOR GROUNDWATER ASSESSMENT IN WEST EL NEGILA AREA, NORTHWESTERN COAST, EGYPT

N.H.T. El-Gendy[1], A.M.A. Youssef[2], A.M.M. Al-Tamamy[2], A.M. El-Sheshtawy[1], S.H. Radwan[2]

(1) Geology Department, Faculty of Science, Tanta University

(2) Desert Research Centre, P.O.B. 11753, Cairo, Egypt

استخدام النمذجة الجيوكهربية والكهرومغناطيسية فى تقييم المياه الجوفيه فى منطقة غرب النجيلة، الساحل الشمالى الغربى، مصر

الخلاصة: إن تقييم المياه الجوفية فى المناطق الجافة مثل منطقة غرب النجيلة بالساحل الشمالى الغربى لمصر ضرورى ومهم من اجل التحضر والتنمية المستدامة, علاوة على ذلك فإن المياه الجوفية تعتبر المصدر الأساسي الذى يمد المنطقة بالمياه اللازمة للشرب والزراعة والتنمية ولذلك فقد تم عمل عدد ٤ جسات جيوكهربية و ٥٠ جسة كهرومغناطيسية لتحديد الوحدات الهيدروجيولوجية بالمنطقة قيد الدراسة. وقد تبين من تفسير قطاعات المسح الجيوكهربى والكهرومغناطيسى أن التتابع السطحى فى منطقة الدراسة يتكون من ٤ طبقات جيوكهربية (أ, ب,ج, د) وتمثل الطبقة الثالثة (ج) الطبقة الحاملة للمياه فى المنطقة والتى تتكون من حجر جيرى مشقق (Marmarica limestone) ذو العمر الجيولوجى الميوسينى الأوسط والتى تتميز بمقاومة متوسطة إلى منخفضة (٨,٨ الى ١٤٠ أوم.م) ويتراوح سمكها من ١٦ الى ٤٠م وتوجد على عمق من ٢ الى ١٦ م . ويتجه سريان المياه الجوفية فى هذه الطبقة من الجنوب الى الشمال فى اتجاه البحر المتوسط . وقد تم تحديد أولوية المنطقة من حيث الكميات المناسبة من المياه الصالحة للاستخدام وذلك طبقا لقيم المقاومة العالية والسمك الأكبر للطبقة الحاملة للمياه. ومن خلاله فقد تم اختيار أفضل أماكن لحفر الآبار والتى توجد معظمها فى المنطقة الجنوبية من منطقة الدراسة حيث أقل ملوحة وأفضل خصاص للمياه.

ABSTRACT: *Evaluation and assessment of groundwater in arid regions such as the West El Negila area along the Northwestern Coast of Egypt is important for urbanization and sustainable development. Therefore, groundwater may become the most reasonable complementary resource that is capable to supply the area with needed water for drinking, agriculture and the development. A number of 4 vertical electric soundings (VES) and 50 time domain electromagnetic (TEM) soundings were carried out to investigate the subsurface hydrogeological units in the study area. The interpretation of VES and TEM revealed that the subsurface succession consists of four geoelectrical layers (A, B, C and D). The geoelectrical layer "C" which is equivalent to the Middle Miocene Marmarica limestone represents the water bearing formation in the study area; it attains moderate to low resistivity values (8.8 - 40 Ω.m) and thickness of 16- 40m and appears at depth 2 -116m underground surface. In general, the groundwater is expected to flow from south to north towards the Mediterranean Sea. The priority of sites to provide significant volumes of potable water was determined according to the relatively high resistivity and thickness of the water bearing layer. The more promising locations for drilling water wells exist in the southern parts of the area of study, where the potential for potable groundwater increases. It is expected that the salinity of water bearing layer increases due north.*

INTRODUCTION

At present, the Northwestern Coastal Zone (NWCZ) of Egypt is attracting the attention of the government and also the investors for future sustainable development. The investigated area represents a part of the Mediterranean coastal zone. It has excellent locality for land reclamation and tourism projects. The needs for land reclamation and water resources development are to improve the poverty in Egyptian farmland and help in feeding the Egypt's expanding population (Pautsch and Abdelrahman, 1998). This development depends principally on the occurrence and continuity of the groundwater resources. Rain water is the main source of water for cultivation, but the amount of water is insufficient. The major challenge that Egypt faces nowadays is the need for better development and management of natural resources, to fulfill the needs of a growing nation.

The present work focuses on the karst aquifer which can be considered as the main aquifer in the Northwestern coastal zone of Egypt which is represented by the Middle Miocene Marmarica limestone. It builds up mainly of fissured and cavernous limestone, with clay and marl intercalations. Principally, the structural setting can be considered as the main factor which controls the groundwater occurrence in the aquifer (Yousif et al., 2015). About 25% of the world's population use Karst aquifers for drinking water resources where it provides important water resources world-wide (Ford and Williams, 2007). Hydrogeophysics has been a growing field in karst hydrology that has been used to improve understanding of the distribution of secondary porosity (McGrath et al., 2002; Sumanovac and Weisser, 2001 and Van Schoor, 2002).

This study provides better information about the geological and hydrological setting of the study area. The main objectives of the present study are the exploration and evaluation of the groundwater occurrence and the detection of the flow and recharge direction. Also, to determine the vertical and horizontal extensions of the lithological succession with their facies characteristics as well as defining the best sites for drilling water wells.

The application of vertical electrical sounding (VES) and time domain electromagnetic (TDEM) are represent the approach of the present study.

LOCATION OF STADY AREA

The area under investigation represents a small part of the Northwestern Coastal Zone (NWCZ) of Egypt. It lays west El Negila city and extends for about 24.5 km along the coast. It is bounded by longitudes 26◦ 15' & 26◦ 30' E, and Latitudes 31◦ 15' & 31◦ 33' N covering an area of about 718 km^2 (Fig.1). The zone of the investigated area is characterized by elevations ranging from 2m to 170m.

CLIMATE

The climatic conditions of the study area are typically arid, characterized by a long hot dry summer, mild winter with little rainfall, high evaporation with moderate to high relative humidity (Yousif et al., 2015). The Mediterranean coastal zone of Egypt receives noticeable amounts of rainfall, especially in winter. In summer, no rain is recorded, while in autumn, occasional heavy rain may occur.

During the period from 1 January 1998 to 1 January 2012, Yousif et al., (2015) found that most parts of El Negila area receive a total precipitation ranging between 2291 mm (annual average 163.64 mm) and 2781 mm (annual average 198.64 mm), in addition to an estimation of the annual precipitation during 1 year (2012), where its maximum value was 196.8 mm.

GEOMORHOLOGICAL, GEOLOGICALAND HYDROGEOLOGICAL SETTINGS

Geomorphological:

On the regional level, four main geomorphological units are differentiated in the area of study: the tableland, the piedmont plain, the coastal plain, and the drainage basins. These units are oriented nearly parallel to the present Mediterranean shore in a nearly E–W direction (Fig. 2). These geomorphological aspects will be discussed from south to north according to many authors, such as: El Shazly, 1964 and 1972; Hammad, 1966; El Shamy, 1968; El Senoussi and Shata, 1969; Selim 1969; Taha, 1973; Misak, 1974; Rizk, 1982; Hammad et al., 1986; Raslan, 1995; Youssef et al., 2015 into the following: ***The tableland*** occupies the southern part of the area of study and is characterized by northwards slopes. The elevation of the tableland is varying between 75 and 125 m above sea level. It represents the main watershed area where its surface is dissected by a series of shallow valleys. The tableland is composed mainly of massive Pliocene and Middle Miocene limestone rocks. It is covered partially by accumulations of aeolian sand dunes.The surface of the tableland area is characterized generally by the development of a hard crust on the top of the weathered surface. This hard crust layer has a thickness that varies between 20 and 40 cm and is composed of dolomitic limestone. Hence, it provides a good chance for accumulation of surface water runoff which is directed to the low land area to the north (Youssef et al., 2015).

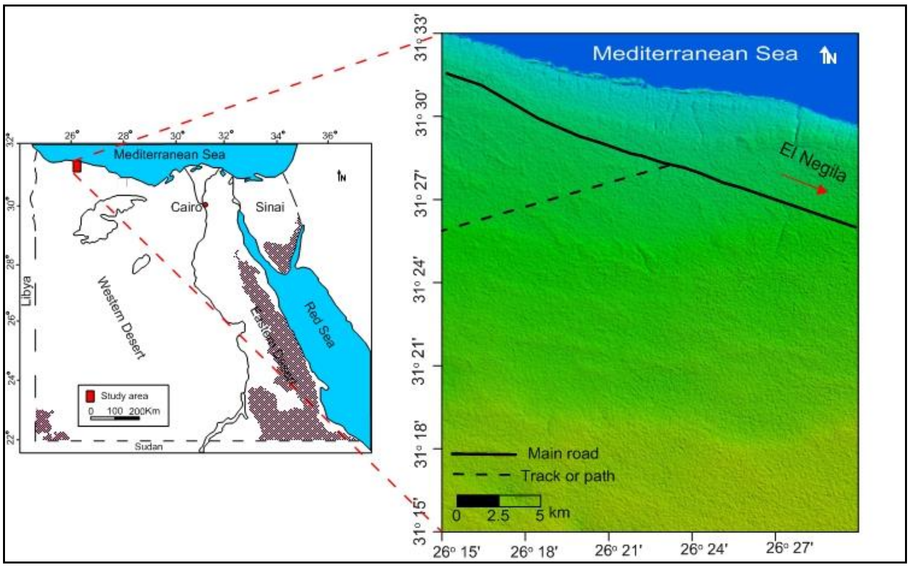

Fig. 1: Location map of the study area.

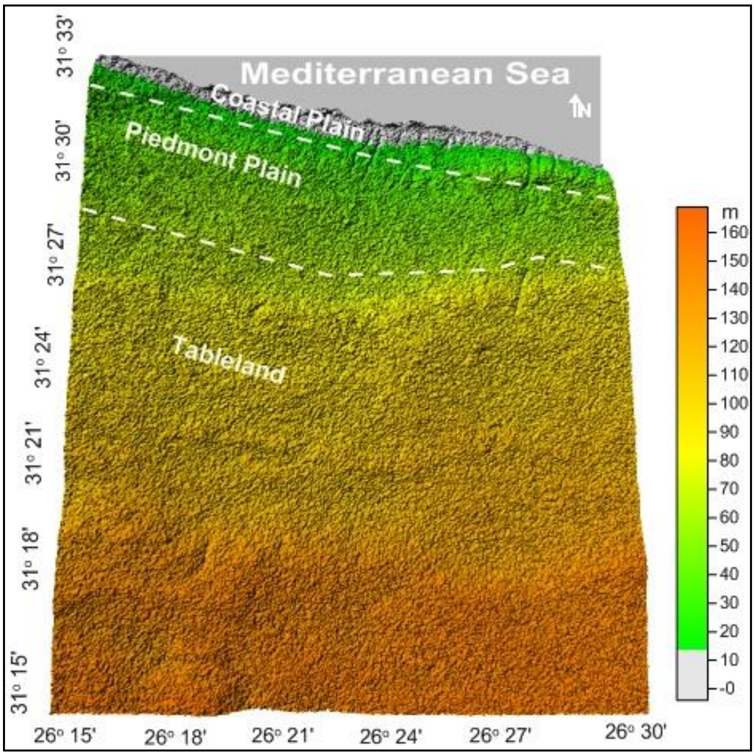

Fig. 2: Geomorphological setting of the study area illustrated in 3D views from DEM

The piedmont plain represents an extended sloped surface separating the southern tableland from the northern coastal plain with elevation ranges between 30 and 90 m above sea level. The width of the piedmont plain varies from few meters to several kilometers. This plain contains inland depressions between the ridges (El Shazly, 1964).This plain has elongated shape and it is characterized by undulated surface. The surface of the plain is either covered with thin layer of alluvial sand deposits or degraded and appears as rocky surface. During the rainy season, the plain receives much of the surface runoff of both the tableland and the most inland ridge. This plain is occupied by subunits as, inland ridges, and depressions. (Yousif et al., 2015).

The coastal plain occupies a narrow strip of land stretching adjacent to the Mediterranean Sea. It is characterized by elevation ranges between 0 and 30 m above sea level and has northward slope. The maximum inland width of this plain is about 5 km from the sea (N_S). The landscape of the coastal plain is influenced by several landforms, which include elongated ridges, dunes and shallow depressions (Raslan, 1995).

Drainage pattern; the basins in the area of interest are generally parallel with main channel streaming from the tableland and flow down towards the Mediterranean Sea according to thegeneral slope of land surface. The area of interest is dissected by three main basins trending S-N direction; namely wadi Shammas in the east, wadi Al Sedrah in the middle and wadi al zowaidah in the west (Fig.3). these wadis are dipping due northward and causes discharge towards the Meditrranean Sea.

Geological setting Stratigraphically, the northwestern coastal zone of Egypt is totally occupied by sedimentary rocks belonging essentially to the Tertiary and Quaternary according to many authors such as Shata, 1955 and 1957; Said, 1962; El Shazly, 1964 and 1972; Hammad, 1966 and 1972; Yousif et al., 2015. Tertiary rocks are exposed on the surface at the southern tableland where they are dissected by several wadis. The Tertiary deposits in the study area are mainly represented by the Middle Miocene sediments which are represented by the Marmarica Formation which is built up of fissured and cavernous limestone, dolomitic limestone, and sandy limestone intercalated partly with marl intercalations. The Quaternary sediments in the study area are mainly represented by Pleistocene and Holocene deposits.

The geological structures of the study area (Fig. 3) can be considered as a part of the main structure, which affects the northwestern coast of Egypt. The Northwestern coastal zone is dominated by folds and faults, with most folds formed during Late Cretaceous-Early Tertiary, and have NE-SW direction that agrees with the Syrian Arc system trend (Shata, 1957 and Said, 1962). The majority of faults are step normal faults which have long history of growth, while the second type of faults are strike slip faults which related to the movement during the late Cretaceous. The faults have NE-SW and N-S trend (Shata, 1955).

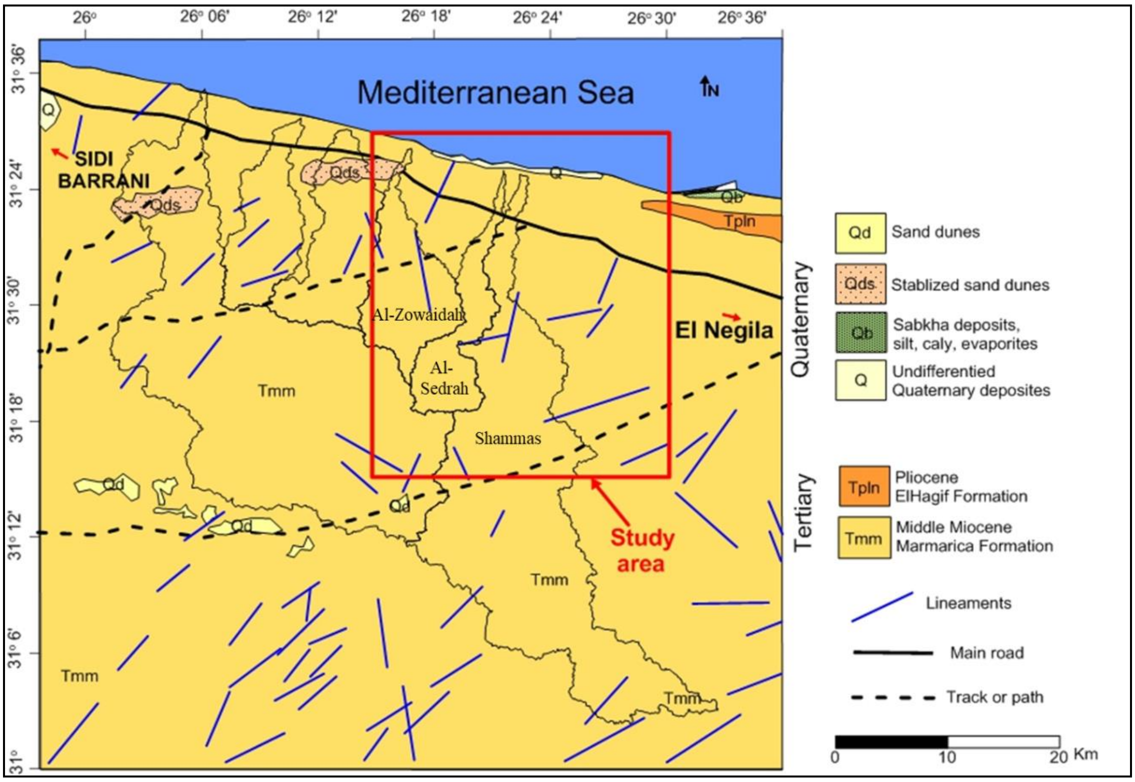

Fig. 3: Geologicalal setting and structural lineaments of the area, (CONOCO, 1987).

Hydrogeologicalal setting

The water resources in different areas along the Northwestern coastal zone have been investigated by: Raslan (1995), Yousif and Bubenzer (2013a and b) and Yousif et al., 2014. The aquifers in the area of study were stratigraphically classified into Pleistocene and Middle Miocene aquifers (Rizk, 1982).

The Pleistocene aquifer is composed of detrital ooltic limestone with thickness of 10 to 75m (Raslan, 1995). The groundwater belonging to this oolitic limestone comes either from direct infiltration of annual rainfall on the oolitic limestone ridges or from rain water falling on the table land region.

The Middle Miocene aquifer is represented by Marmarica limestone aquifer which consists of alternating beds of limestone and clay. The limestone is highly fissured and jointed (Raslan, 1995).

DATA ACQUSITION AND METHODOLOGY

Field work

The geophysical field works involved the application of three different techniques involving; vertical Electrical sounding (VES) and time domain electromagnetic (TEM) for the purpose of detecting the depth to water bearing layer, the horizontal and vertical lithological variations, the thickness of the fractured limestone water-bearing and fracture characteristics and geometry if available. A total number of 4 VES stations and 50 TEM stations (Fig. 4) are carried out in the area of interest. The location of VES and TEM stations has been chosen according to the accessibility and the filed conditions. Each of these geophysical methods is discussed separately as follows:

Vertical Electrical Soundings (VES)

Vertical electrical soundings are applied to a horizontally or roughly horizontally stratified earth. The aim of this technique is to observe the vertical variations within the electrical resistivity of the subsurface layers. The Schlumberger electrode array has been utilized for the data acquisition in the present work. During this array four electrodes (A, B, M and N) took a systematic configuration in a straight line where the current and potential electrodes have a common mid-point. Four vertical electrical soundings (VES) conducted in the area of study (Fig. 4) by using the Schlumberger array with a maximum AB/2 spacing ranging between 700 m and 1000 m. At each sounding station, the apparent electrical resistivity was measured against half the current electrode spacing (AB/2) and plotted on log /log scale in the form of field resistivity sounding curve. The geoelectrical measurements were carried out by using SYSCAL JUNIOR Switch-72. VES number 1 was carried out besides a well to benefit from its available data such as the depth to the fractured limestone water-bearing and thickness of the water– bearing layer in the constructed initial model as well as the vertical lithological variation in the model. **Time Domain Electromagnetic (TEM)** A number of 50 TEM stations (Fig. 4) were carried out using the TEM- fast 48 conductivity meter with loop size 25m, 100m and 200m according to the topography of the area.

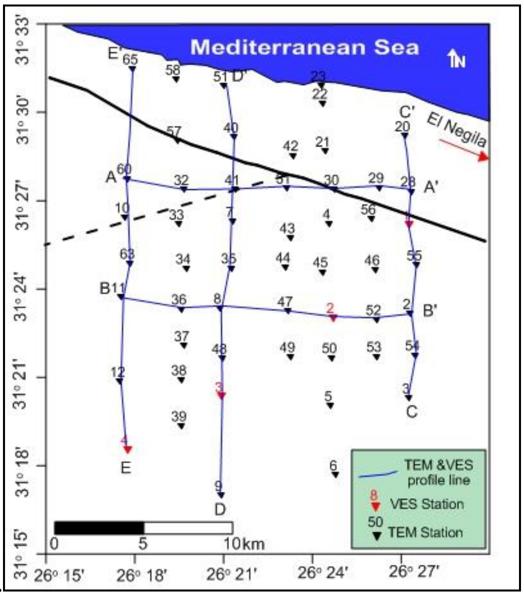

Fig. 4: A map showing the locations of VES, TEM sounding stations, profile lines and 2-D ERT profiles in the area.

TEM survey in this study adopted a single loop configuration in which signals are transmitted and received utilizing the same loop (Fitterman and stewart, 1986) at each station. The survey was repeated several times to enhance the signal noise ratio and the measurements were selected with less noise for the modeling and interpretation. TEM 1 was carried out beside a well and has the same location of VES1 to benefit from the available data of the well in the construction of the initial model and comparing the results of VES1 and TEM1.

RESULTS AND DISCUSSION

1-D geoelectrical and electromagnetic

The measured resistivity data was interpreted in qualitative and quantitative approaches. The qualitative interpretation of the VES includes description of all curve types and constructing on aerial distribution map to compare the relative changes in the apparent resistivity and thicknesses of the different layers detected on the sounding curves. It gives information about the types of curves, number of layers and their continuity throughout the area along a certain direction or through the whole area which, in turn, reflects the degree of homogeneity or heterogeneity of the individual layers. The quantitative interpretation of the geoelectrical resistivity sounding data was carried out using two softwares; the first is the computer software RESIST developed by Van Der Valpen (1988) and the second is utilizing the obtained inversion from RESIST as an initial model for the IX1D program. This quantitative interpretation is used to obtain true resistivity values and the corresponding thicknesses of the geoelectrical layers for each sounding. Figure (5) illustrates the interpreted sounding curves of the four vertical electrical soundings (VES), where the apparent resistivity values were plotted in a log-log scale. These sounding curves seem to be similar in resistivity behavior across the area of interest. The processing and interpretation of the TEM data were also carried out by using the IX1D program. To obtain more realistic results, a geoelectrical and TEM soundings were carried out at the same location and beside a borehole to increase the precise and the accuracy of the interpretation of the field data. The data of the borehole was used as a guide in the construction of the initial models in the interpretation of both the VES and the TEM data (Fig. 6). The interpretation of VES No.1 and TEM No. 1, which were constructed at the same location, show approximately the same inversion model with the number of layers, the same thickness of layers and small change in the resistivity values (Fig.7). According to this significant match with the outcomes of the vertical electrical sounding and the time domain electromagnetic sounding, the interpretation of the other VES and TEM soundings were done without using the joint inversion method.

The results of quantitative interpretation of both the geoelectrical and TEM data revealed that the geoelectrical succession consists of four geoelectrical layers; A, B, C and D. The vertical and horizontal distribution of these geoelectrical layers were clarified through the construction of six geoelectrical cross sections to establish the geological and the hydrogeological situation in the area of interest and to give an ideal picture about the homogeneity and heterogeneity of the lithological units. The cross-sections A-A' and B-B' traverse the area in W-E direction (Figs. 8 and 9), while cross-sections C-C', D-D', E-E' and F-F' are constructed in S-N direction (Figs.10-13).

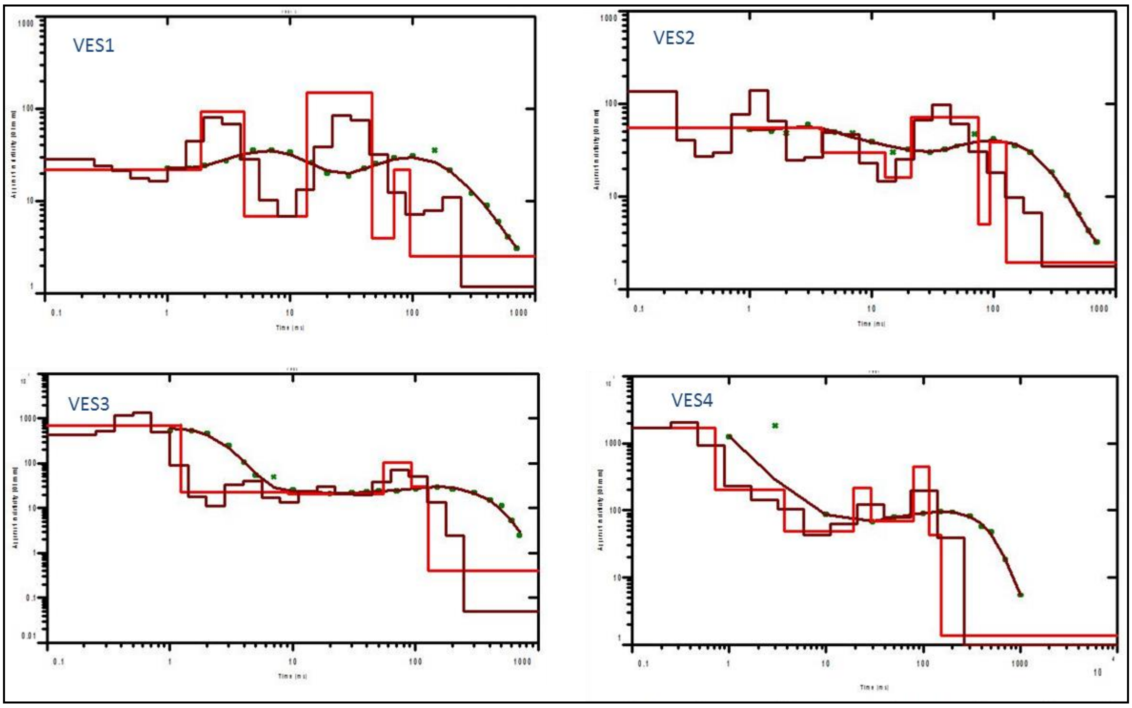

Fig. 5: 1-D VES Data Inversion of four sites considered using IX1D program.

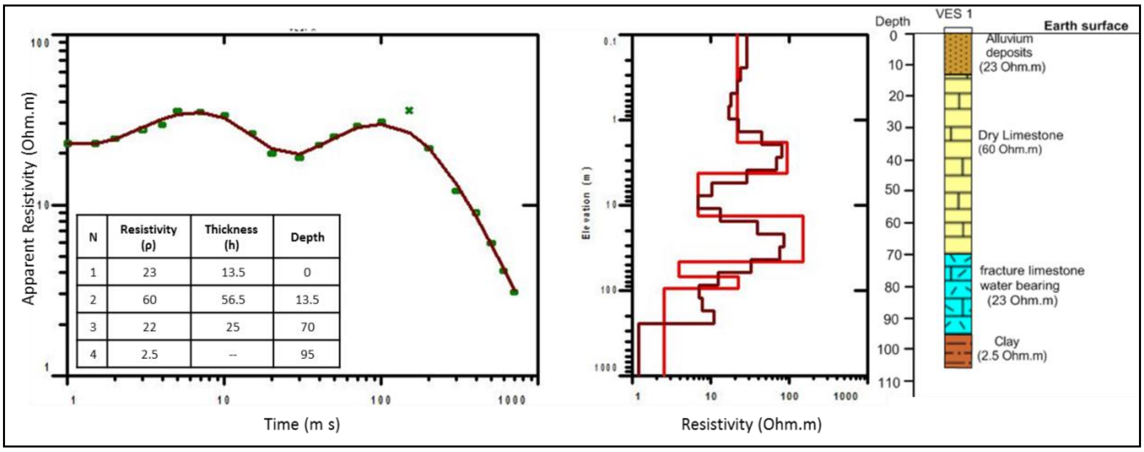

Fig. 6: Interpretation of VES No. 1 using 1-D forward modeling (1x1d V3 program) and the borehole data

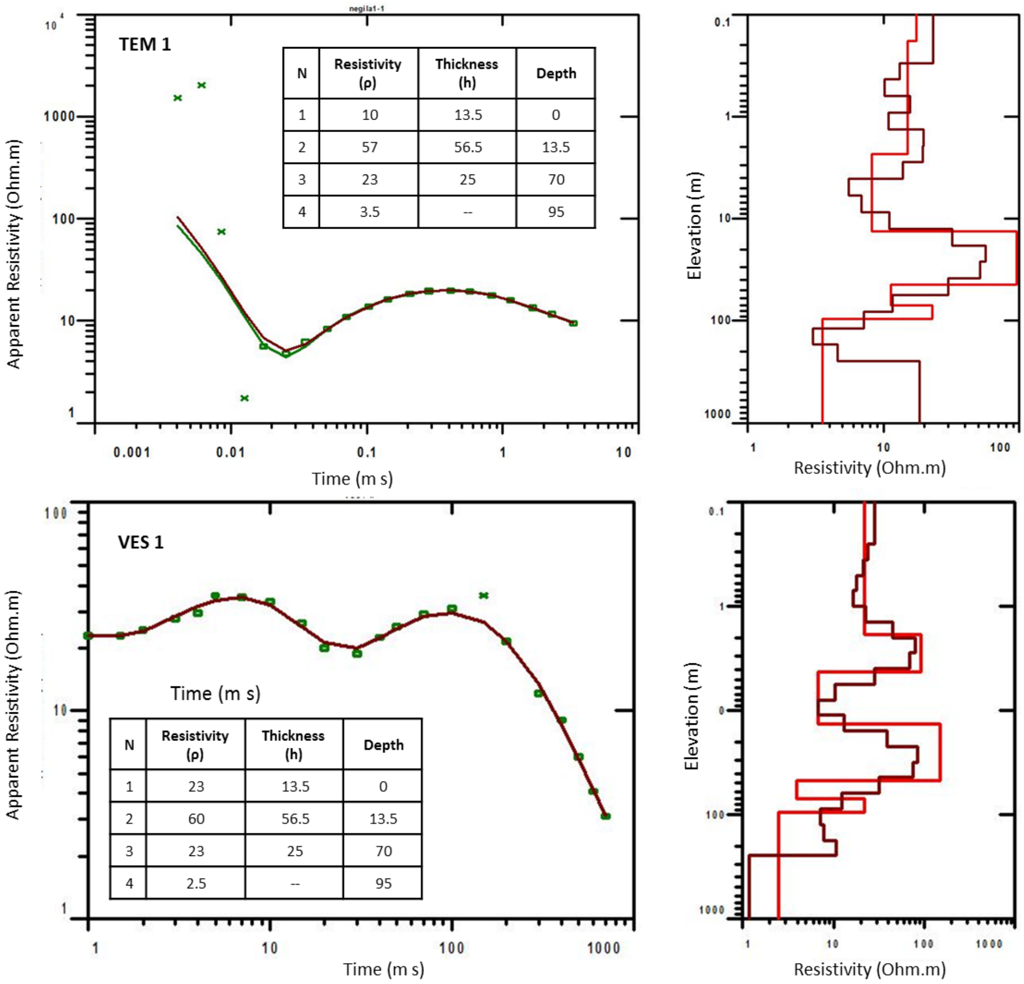

Fig. 7: justifying the interpretation models for both TEM No.1 and VES No. 1 using the IX1D program

These obtained cross sections from VES and TEM data indicate that the area of study is characterized by similar lithological and hydrological conditions. All the cross sections show four geoelectrical layers with similar range of resistivity values but the thicknesses of the layers change from south to north direction as shown in cross sections and in table (1).

The main details of the obtained geoelctrical layers of these cross sections can be illustrated as follows:

1. The first geoelectrical layer (A) is composed of a group of minute sub-layer and collected in one layer. This layer has resistivity values ranging between 7.8 Ω.m at TEM No.28 and 125 Ω.m at TEM No. 63. The low resistivity values correspond to clay deposits whereas the high resistivity values correspond to dry sand and gravels. The thickness of this layer ranges from 2m (TEM No. 23) to 30 m at VES No.4. This layer corresponds to Quaternary alluvium deposits.
2. The second geoelectrical layer (B) has a wide range of resistivity values. It ranges from 11 Ω.m (TEM No.51) to 468 Ω.m (TEM No.3). The low resistivity values correspond to clay to marly limestone deposits whereas; the relatively high resistivity corresponds to dry massive limestone. The thickness of this layer ranges between 18 m (TEM No. 23) and 87 m (TEM No. 9). This layer (dry limestone) is absent at TEM No. 22 and TEM No. 23 where the water level appears at the mean sea level, so the dry limestone seems to be fully saturated under these stations.
3. The third geoelectrical layer (C) lies beneath the second geoelectrical layer (B). The resistivity of this layer is between 8.8 Ω.m (TEM No. 23) and 40 Ω.m at VES No.4. This layer represents the main aquifer in the study area (fractured Marmarica limestone). The variation in resistivity values of this layer may be related to the variation of salinity and /or intrusion of clay with fractured Marmarica limestone water-bearing. The thickness of this layer varies from 16m (TEM No. 23) to 40 m (VES40).

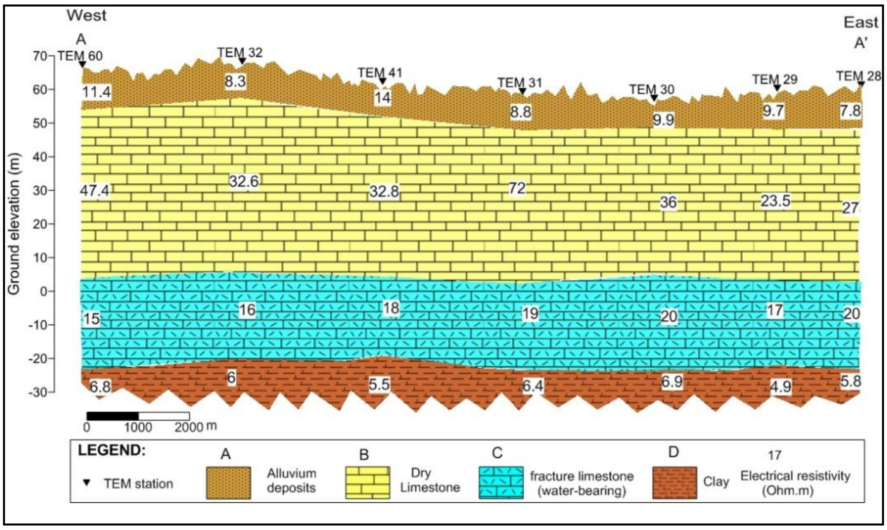

Fig. 8: Geoelectrical cross-section A-A' in W-E direction across the area.

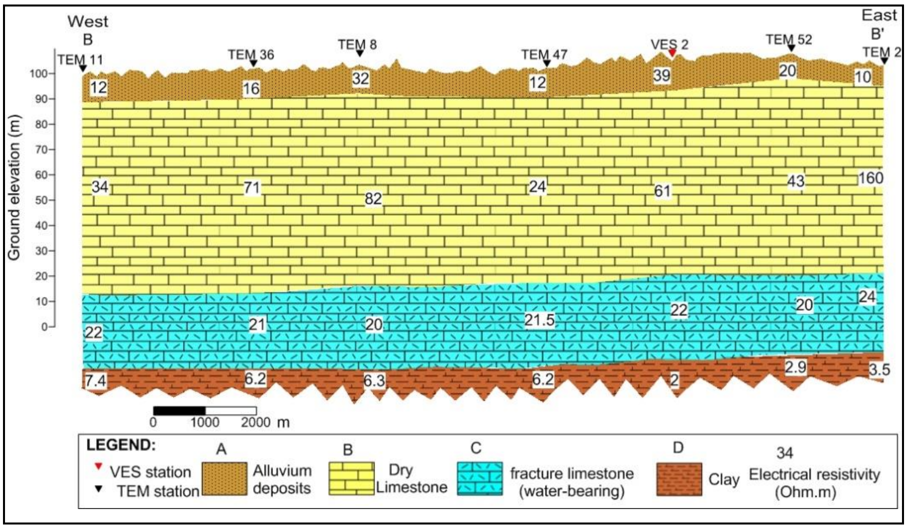

Fig. 9: Geoelectrical cross-section B-B' in W-E direction across the area.

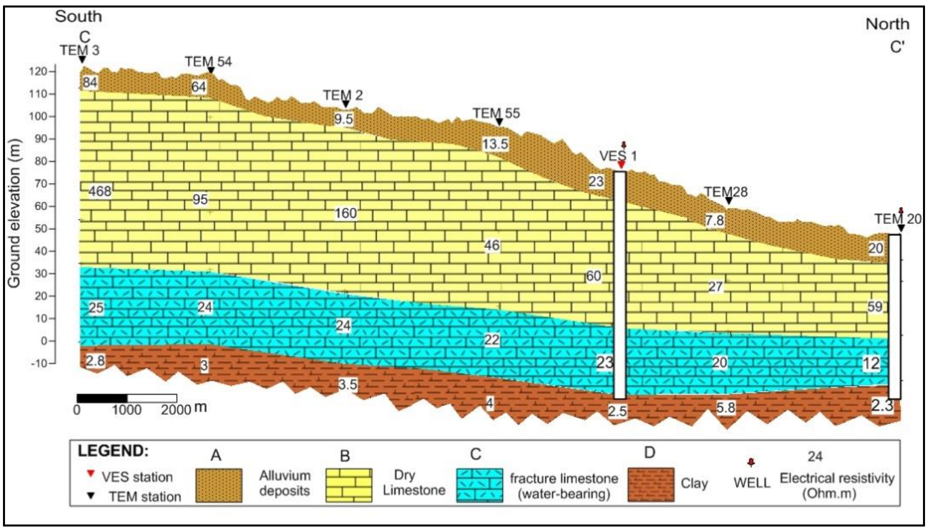

Fig. 10: Geoelectrical cross-section C-C' in S-N direction across the area.

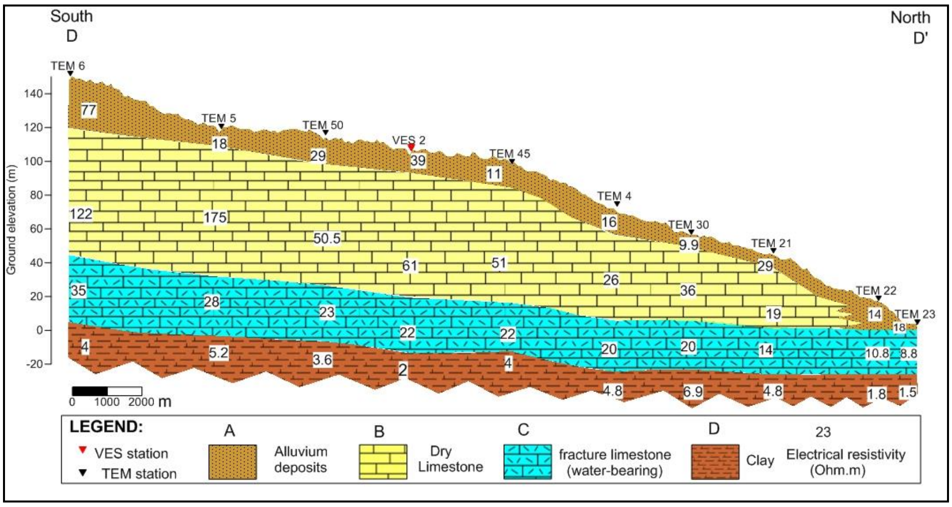

Fig. 11: Geoelectrical cross-section D-D' in S-N direction across the area.

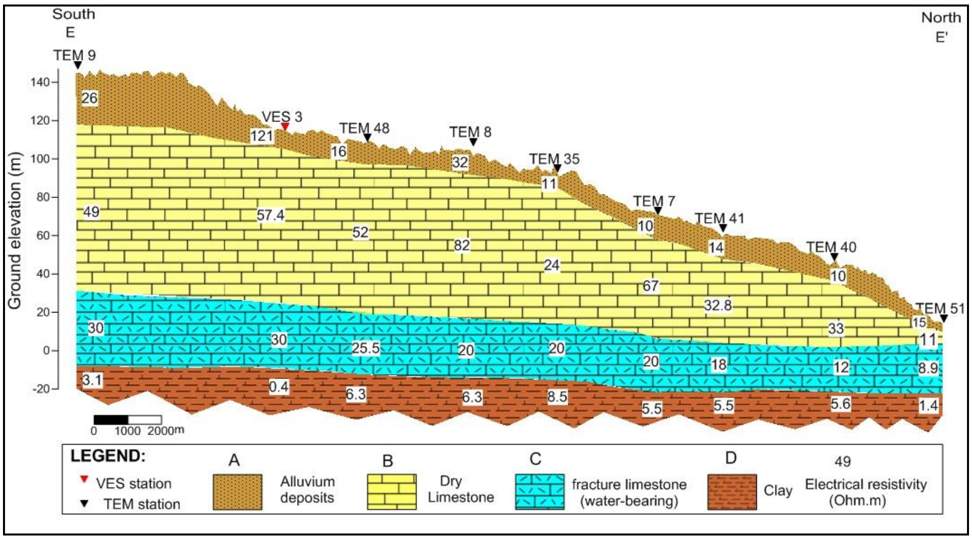

Fig. 12: Geoelectrical cross-section E-E' in S-N direction across the area.

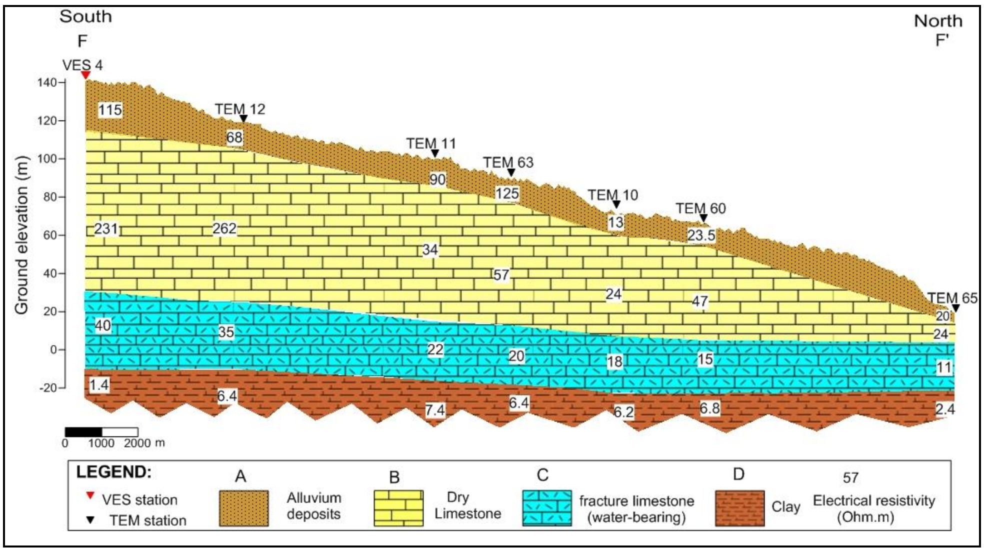

Fig. 13: Geoelectrical cross-section F-F' in S-N direction across the area.

Table 1: Geoelectrical and geological parameters for each study section

Sections	Trend and Length	Geoelectrical layers Resistivity and thickness			
		Layer (A)	Layer B	Layer C	Layer D
A-A'	W-E 15.2 km	7.8-14 Ω.m 6.5-12 m	23.5-72 Ω.m 44-51.5 m	15-20 Ω.m 26-27 m	4.9-6.9 Ω.m ------------
B-B'	W-E 15.6 km	10-39 Ω.m 8-13 m	24-160 Ω.m 73-80 m	20-24 Ω.m 30-33 m	2-7.4 Ω.m ------------
C-C'	S-N 16.4 km	7.8-84 Ω.m 8-12m	27-468 Ω.m 24-78m	12-25 Ω.m 20-35m	3.5- 5.8 Ω.m ------------
D-D'	S-N 24.4 km	99- 77 Ω.m 2- 30 m	19- 175 Ω.m 18- 74 m	8.8- 35 Ω.m 15.6- 40 m	1.5- 6.9 Ω.m ------------
E-E'	S-N 25.7 km	10-121 Ω.m 7-29.5 m	11-82 Ω.m 18.6-87 m	8.9-30 Ω.m 17-40 m	0.4-8.5 Ω.m ------------
F-F'	S-N 24 km	10- 125 Ω.m 8.4- 30 m	24- 262 Ω.m 23- 84 m	11- 40 Ω.m 19- 40 m	1.4- 7.4 Ω.m ------------

4. The fourth geoelectrical layer (D) represents the base of the aquifer. It is characterized by relatively low resistivity values varying from 0.4 at VES No. 3 to 8.5 Ω.m at TEM No.35. This layer corresponds to clay deposits. The lower bottom of this layer was not detected with the used current electrodes separation.

Groundwater occurrence

According to geophysical measurements, it can be noted that the groundwater aquifer in the area of concern represented by Middle Miocene Marmarica Formation which consists of fractured limestone (geoelectrical layer "C"). To study the characteristics of the water bearing formation as well as giving an idea about the groundwater occurrences, the following maps are constructed and discussed (Figs. 14-17):

Isoresistivity contour map of the water bearing layer"C":

The resistivity value at each VES and TEM station was used to illustrate the aerial distribution of the resistivity of the water bearing formation along the investigated area (Fig. 14). This map shows that the resistivity values has a general trend of decrease northward which reflects the increase of the water salinity in the same direction towards the sea. The resistivity ranges between 8.8 at TEM No.23 at the north and 40Ω.m at VES No.4 at the south.

Isopach contour map of the water bearing layer"C'':

Figure (15) illustrates the aerial distribution of the thickness of the water bearing formation along the investigated area The thickness of the water bearing formation varies from 16 m (TEM No. 23) at the north to 40 m (TEM No.6, TEM No. 9, TEM No. 39 and VES No. 4) at the south with a general increase southward.

Depth to water bearing formation layer "C":

The water surface in the area of study appears within the investigated depth of 2-116m, where the minimum recorded depth is 2 m (TEM No. 23) at the north and the maximum recorded depth is 116 m (TEM No. 39) at the south. This wide range variation in depth is attributed mainly to the variation of the topography, as the ground elevation of the study area varies between 2 m in the northern parts (at the coastal plain) and 146 m in the southern parts (at the tableland). Figure (16) revealed that the depth to the top of the fractured Marmarica limestone water-bearing (Geoelectrical layer C) increases mostly southwards.

Level of top surface of water bearing layer "C":

The level of the top surface of water bearing formation with respect to mean sea level can be considered as the water level in the area of study. The geophysical results revealed that the water level ranges from the mean sea level at the northern parts (TEM No. 22 and TEM No. 23) to 45m above mean sea level at the southern parts (TEM No. 6) within general northward decreases. These values give an idea about the general water flow and aquifer recharge. As shown in Figure (17), the water flow is from highest values at the south to the lowest values at the north towards the coastal area and the sea. Also, the groundwater recharge is from the highest values at the south (at the table land) which represents the upstream of the different wadies to the lowest values at the north which is represents the downstream and the deltas of the wadies at the coastal area.

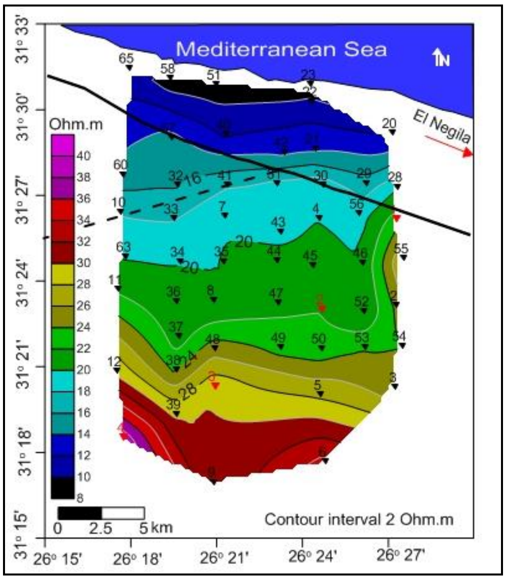

Fig. 14: Iso-resistivity contour map of the water bearing layer in the study area

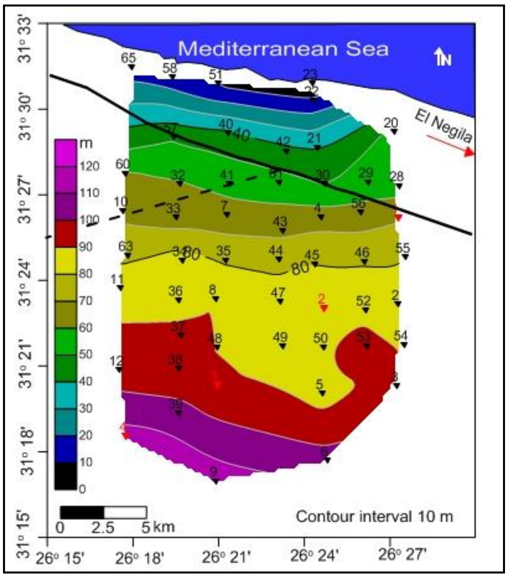

Fig. 15: Iso-pach contour map of the water bearing layer in the study area

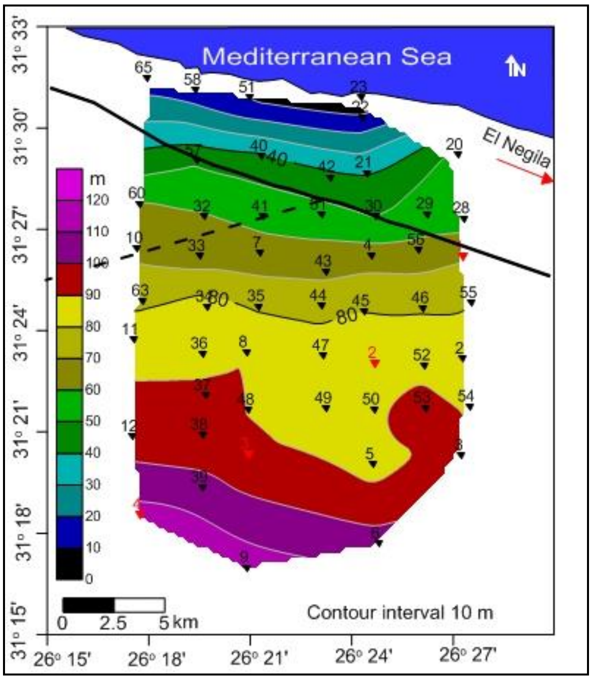

Fig. 16: Contour map of depth to water bearing layer in the study area.

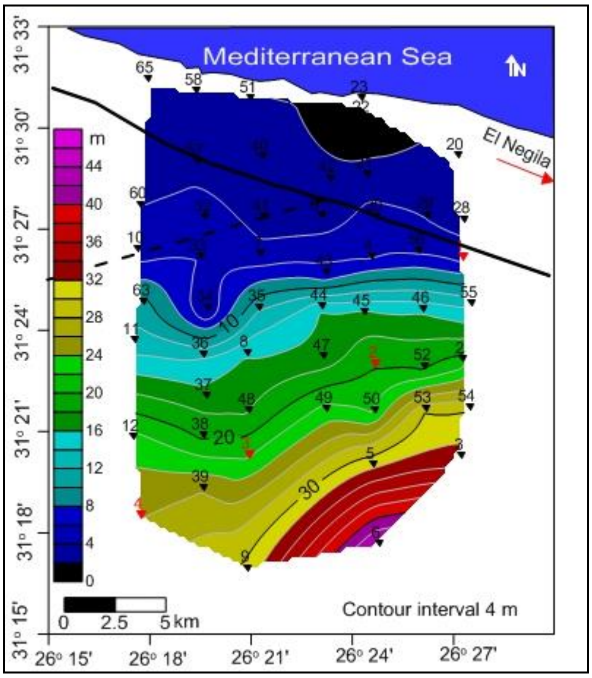

Fig. 17: water level contour map in the study area.

CONCLUSIONS

Geophysical data revealed that the main aquifer in West El Negila area is the Marmarica limestone which consists of fracture limestone. Resistivity map shows that groundwater in the southern parts of the area might be of good quality than that in the northern parts. The thickness of the aquifer increases towards the south. Hence, the most appropriate areas for drilling new water wells possess the southern zone of the study area. Also, the water level map revealed that the groundwater flow from the south to the north with general northward direction towards the Mediterranean Sea.

REFERENCES

CONOCO, 1986: Geological map of Egypt, scale 1:500,000 GPC, sheets No. NH35NE (Alexandria) and NH35NW (El-Sallum).Interpex Limited, 1993. RESIX-PLUS, resistivity data interpretation software, Golden, Colorado, USA V.2, p. 20.

El Senussi, M.Y. and Shata, A., 1969: Geomorphological and morphological aspects of Umm El Rakham. Bull Inst Desert 19(z):1–32, Cairo, Egypt.

El Shamy, I.Z., 1968: The geology of water and soil resources in El Dabaa area, western Mediterranean coastal zone, U.A.R., M. Sc, Thesis, Fac. Sci ., Cairo Univ., Egypt, pp. 112.

El Shazly, **M., 1964:** Geology, pedology and hydrology of Mersa Matruh area, Western Mediterranean littoral U.R. Unpub., Ph.D. thesis, Fac. Sci. Cairo univ., Cairo, Egypt p2-36.

El Shazly, M., 1972: Contribution to the geochemistry of the groundwater in Mersa Matruh area, Western Mediterranean Coastal Zone, Egypt. Desert Inst Bull XX(2):289–300

Fitterman, D.V. and Stewart, M.T., 1986: Transient electromagnetic sounding for groundwater. Geophysics, Vol, 51, pp. 995-1005.

***Ford*, D.C. and *Williams*, P.W., 2007:** Karst hydrogeology and geomorphology, John Wiley and Sons Ltd., 562 pp. Published in Cave and Karst Science 34 (1) 40-41.

Griffiths, D.H. and Barker, R.D., 1993:Two-dimensional resistivity imaging and modeling in areas of complex geology: Journal Applied Geophysics, v. 29, no. 3, pp. 211–226.

Hammad, F.A., 1966: The geology of water supplies in Ras El Hekma area, western Mediterranean coastal zone, Egypt, M.Sc. Thesis, Fac. Sci. Cairo Univ., Egypt, 109 pp.

Hammad, F.A., 1972: The geology of soils and water resources in the area between Ras El Hekma and Ras El Rum (Western Mediterranean Littoral Zone, Egypt). Ph.D. Dissertation, Fac. Sci., Cairo University

Hammad, F.A., Taha, A.A. and Shata, A.A., 1986: The study of landforms in the area between Ras El Hekma and Ras Alm El-Rum (Northwestern Mediterranean littoral zone, Egypt). Bull Fac Sci 13(1):189–210, Mansoura University

McGrath, R., Styles, P., Thomas, E. and Neale, S., 2002: Integrated high-resolution geophysical investigations as potential tools for water resource investigations in karst terrain. Environ Geol 42:552–557. doi:10.1007/s00254-001-0519-2

Misak, R., 1974: Geomorphology and geology of the area between El Daba'a and Ras El Hekma, Western Mediterranean coastal zone, Egypt. M.Sc. Thesis, Ain Shamas University

Pautsch, G.R. and Abdelrahman, A. H., 1998: Effects of Egyptian economic reforms: the horticultural sector. Food Policy 23(2):199–210

Raslan, S.M., 1995: Geomorphologicalal and hydrological studies on some localities along the Northwestern Coast of Egypt. M.Sc. thesis, fac. of Sci. Menoufia Univ.

Rizk, Z.E., 1982: Geologicalal and hydrological studies on the Northwestern coast of Egypt., unpub. M. Sc. Thesis, Fac. of Sci. Menoufia Univ. Egypt. P 52-70.

Said, **R., 1962**: The geology of Egypt. Elsevier publ. Co., Amsterdam, New York, p. 377.

Shata, A., 1955: An introduction note on the geology of the northern portion of the Western Desert of Egypt. Bull. Inst. Desert. D'Egypte, vol. 5, no. 3, pp. 96-106.

Shata A., 1957: Geology and geomorphology of Wadi El Kharruba area, Western Desert, Mediterranean Littoral, Matruh District, Egypt. Bull. Inst. Desert. D'Egypte, vol. 1, no. 10, pp. 91-120.

Šumanovac, F. and Weisser, M., 2001: Evaluation of resistivity and seismic methods for hydrogeologicalal mapping in karst terrains: Journal of Applied Geophysics, 47, 13-28.

Van Der Velpen, B.P.A., 1988: RESIST version 1.0 a package for the processing of the resistivity sounding data. M.Sc. Research project. ITC, Delft, the Netherlands.

Van Schoor, 2002: Detecting of sinkholes using 2D electrical resistivity imaging. Journal of Applied Geophysics, 50, pp. 393-399

Yousif, M. and Bubenzer O., 2013a: An integrated approach for groundwater assessment at the Northwestern Coast of Egypt (Ras El Hekma area): case study. Springer Environ Earth Sci 69 (7):2227–2246

Yousif, M. and Bubenzer, O., 2013b: Integrated remote sensing and GIS for surface water development. Case study: Ras El Hekma area, northwestern coast of Egypt. Arab J Geosci 6 (4):1295–1306

Yousif, M., Oguchi, T., Anazawa, K. and Ohba, T., 2014: Geospatial information and environmental isotopes for hydrogeologicalal evaluation: Ras Alam El Rum Northwestern coast of Egypt. Nat Resour Res. doi:10.1007/s11053-014-9252-x

Yousif, M., Oguchi, T., Anazawa, K. and Ohba, T., 2015: Framework for investigation of karst aquifer in an arid zone, using isotopes, remote sensing and GIS applications: the Northwestern Coast of Egypt. Environ. Process. 2:37-60 DOI 10.1007/s 40710-015-0063-9.